Study, simulation and realization of a fuzzy logic-based MPPT controller in an isolated DC microgrid

Abdelaziz Youssfi[1], Abdelmounaim Alioui[2], Youssef Ait El Kadi[1,3]

[1]Engineering and Applied Physics research team (EAP), High School of Technology, Sultan Moulay Slimane University, Beni Mellal, Morocco

[2]Laboratory of Industrial Engineering and Surface Engineering, Faculty of Sciences and Technologies, Sultan Moulay Slimane University, Beni Mellal, Morocco

[3]Higher School of Technology, Sultan Moulay Slimane University, Beni Mellal, Morocco

Article Info

ABSTRACT

This study presents a pioneering methodology for implementing the maximum power point tracking (MPPT) controller, based on fuzzy logic. Through a comprehensive performance analysis, we evaluate its effectiveness compared to the widely used perturb and observe (P&O) algorithm, which is a common MPPT technique. The main objective of our proposed MPPT approach is to improve the performance of a photovoltaic (PV) system. To evaluate the performance of the proposed MPPT controller and compare it with the P&O algorithm, we designed and simulated both controllers using MATLAB/Simulink. We also implemented a prototype of the controllers using an Arduino Mega board, and evaluated their performance under real operating conditions. The experimental results unequivocally confirm that the fuzzy logic-based MPPT controller outperforms the P&O algorithm in terms of performance, speed and accuracy. The fuzzy logic controller offers greater accuracy in tracking the maximum power point under various environmental circumstances, including variations in solar irradiation and connected load. Overall, this work contributes to the development of efficient and reliable MPPT controllers for PV systems, and provides a comparison of the performances of two popular MPPT techniques. Future research could explore other MPPT techniques and evaluate their performance using similar experimental setups.

Corresponding Author:

Abdelaziz Youssfi
Engineering and Applied Physics research team (EAP), High School of Technology
Sultan Moulay Slimane University
Beni-Mellal, Morocco
Email: abdelaziz.youssfi@usms.ma

1. INTRODUCTION

In today's world, the demand for energy is growing all the time, but conventional energy sources are rapidly running out. Otherwise, conventional sources have a major impact on the environment, as their use leads to carbon dioxide (CO_2) emissions [1]. For this reason, researchers are finding new sources that are just as natural, less CO_2-emitting, and more sustainable [1]–[3]. These sources include photovoltaics (PV), wind turbines, and green hydrogen [4], [5]. This study focuses on the PV source, based on the PV effect, a process discovered in 1839 by French physicist Alexandre Edmond Becquerel [6]. It is a physical phenomenon resulting from the interaction between solar radiation and matter, which generates an electric current [6], [7]. A PV source is necessarily non-linear, it is operation depending on several factors such as irradiation,

temperature and the connected load [8], [9]. So, a PV source is not capable of producing maximum power if any of its parameters change when connected directly to the load. For this reason, researchers have developed a maximum power point tracking device called MPPT, based on the concept of optimization algorithms. An intermediate stage is then added between the PV source and the load, containing the MPPT power optimization device and a power converter, generally of the DC-DC type. There are several types of MPPT algorithms, differing in complexity, speed and performance [10]. The system we are going to study is illustrated in Figure 1, we want to maximize the power of a solar system in an isolated DC microgrid. This microgrid can in fact be an isolated DC installation, such as an isolated street lighting station, or an isolated AC installation injecting an inverter instead of the DC load, such as an isolated solar pumping station.
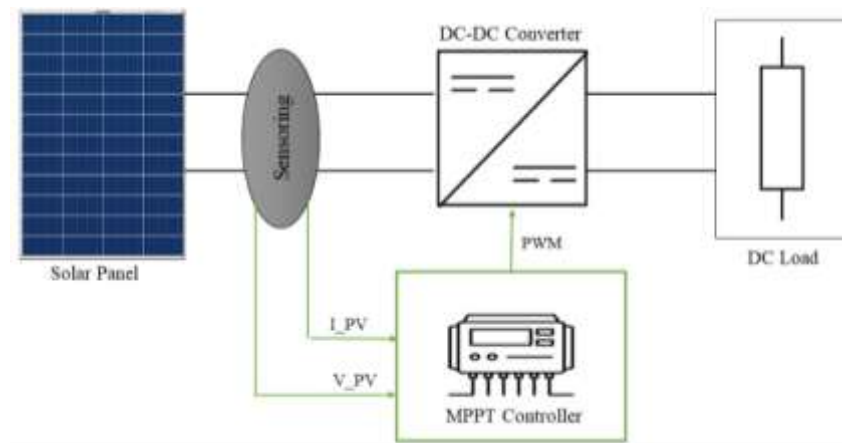

Figure 1. Diagram illustrating a photovoltaic system with MPPT controlled static converter [10]

In this context, some of the most widely used MPPT algorithms are cited [11]. The perturb and observe (P&O) algorithm is the most frequently used because of its ease of implementation [10]. However, the INC (conductance increment) algorithm is also more widely used in major projects, and is closer in consequence to the P&O algorithm, but its performance may differ from that of P&O [10], [12]. In addition, there are two other types of algorithms that have the same concept. The first is the fraction of voltage (FCO) algorithm, and the second is the fraction of current (FCC) algorithm [11], both of which are simpler to implement, but have lower performance than P&O and INC [11], [13]. Otherwise, the researchers exploited advanced, robust and intelligent algorithms such as the sliding mode (SM) algorithm [14], [15], the fuzzy logic controller (FLC) algorithm [9], [16], the particle swarm optimization (PSO) algorithm [17]−[19] and the artificial neural network (ANN) algorithm [20].

In this work, we propose to study two types of MPPT algorithms of different concept, the first is the P&O algorithm which belongs to the category of classical algorithms, and the second is the FL algorithm which belongs to the category of intelligent algorithms. We used a DC-DC-boost converter, the choice of which is based on the operating conditions of the load connected at the output and the conditions required by the PV system at the input. In the intermediate stage of the system studied, it is necessary to add a suitable power converter, for power maximization by the MPPT method, the major works are using DC-DC converters [21]−[23], there are also other works that are using DC-AC converters [24]. Generally, the choice of converter is determined by the specifications. Our aim is to compare the performance of these two algorithms under different system operating conditions, and to provide engineers and researchers with information on the implementation of fuzzy logic in MPPT controllers.

2. SYSTEM ELEMENT MODELING
2.1. Solar panel modelling
A solar panel is a non-ideal current source which has non-linear characteristics [8]. The energy production of a PV system is essentially based on the PV effect [6], which is a phenomenon of the interaction between photons and electrons in semi-conductor matter [7]. The equivalent diagram of a PV system is modelled as a current generator in antiparallel with a diode and a shunt resistor, and another resistor in series, the Figure 2 illustrates the equivalent model of our system [8].
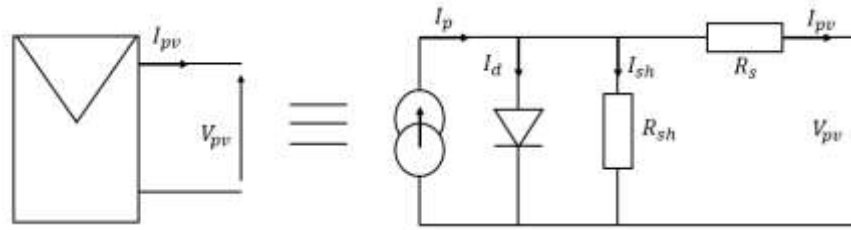
Figure 2. Equivalent electrical model of a photovoltaic panel [8]

To extract the characteristics of a PV system, we need to find a relationship between the current I_{pv} and the voltage V_{pv} [8]. According to the equivalent diagram, we have:

$$I_p = I_d + I_{sh} + I_{pv} \tag{1}$$

$$I_{sh} = \frac{V_{pv} + R_S I_{pv}}{R_{sh}} \tag{2}$$

$$I_d = I_0 \left(e^{\frac{V_{pv} + R_S I_S}{n V_T}} - 1 \right) \tag{3}$$

$$I_p = I_0 \left(e^{\frac{V_{pv} + R_S I_S}{n V_T}} - 1 \right) + \frac{V_{pv} + R_S I_{pv}}{R_{sh}} + I_{pv} \tag{4}$$

finally:

$$I_{pv} = I_p - I_0 \left(e^{\frac{V_{pv} + R_S I_S}{n V_T}} - 1 \right) - \frac{V_{pv} + R_S I_{pv}}{R_{sh}} \tag{5}$$

This equation can be used to determine the characteristics of a solar panel if its parameters are known. In general, the characteristics of a PV system are given in the Figure 3, Figure 3(a) represents I_{pv}-V_{pv} characteristics, Figure 3(b) represents P_{pv}-V_{pv} characteristics. It is obvious then that the characteristics of a PV system are necessarily non-linear, so the optimum operating point is more sensitive to variations in the connected load or irradiation.
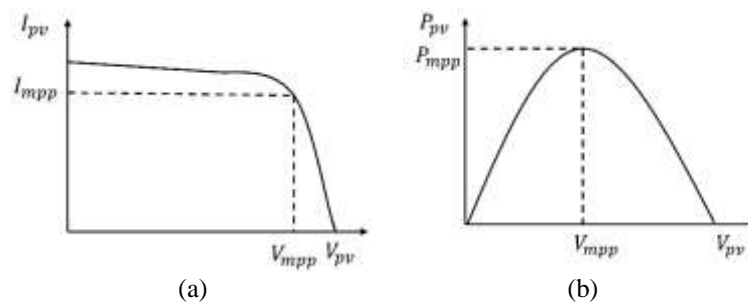

| (a) | (b) |

Figure 3. PV source characteristics (a) I-V characteristic and (b) P-V characteristic [8]

2.2. Boost converter modelling

A boost converter is a meticulously crafted DC-DC converter with the precise objective of elevating the voltage level originating from a DC power source [25]. Its functioning is grounded in a fundamental principle whereby energy is judiciously stored in an inductor upon application of the input voltage. Subsequently, the accumulated energy is cautiously released to the output during the off-time of the switching cycle. The Figure 4 shows the boost converter circuit used in this work.
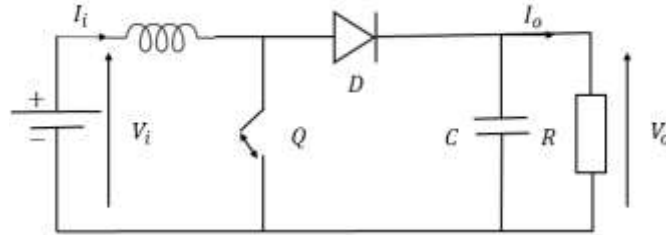
Figure 4. Boost converter circuit diagram [25]

This meticulous process ultimately culminates in the production of an output voltage that surpasses the initial input voltage, effectively achieving voltage amplification and meeting the desired voltage requirements [26]. The proposed mathematical model using the following approximations [25]: i) the transient regime is not taken into account, ii) the components are assumed to be ideal, and iii) study in continuous conduction mode. Our converter operates in two modes depending on the state of switch Q. The Figure 5 illustrates these two modes of operation. Figure 5(a) as boost converter equivalent circuit in ON mode, and Figure 5(b) as boost converter equivalent circuit in OFF mode. The Figure 6 shows the current and voltage behavior in a boost converter switching period, Figure 6(a) represents the inductor current and Figure 6(b) represents the inductor voltage.
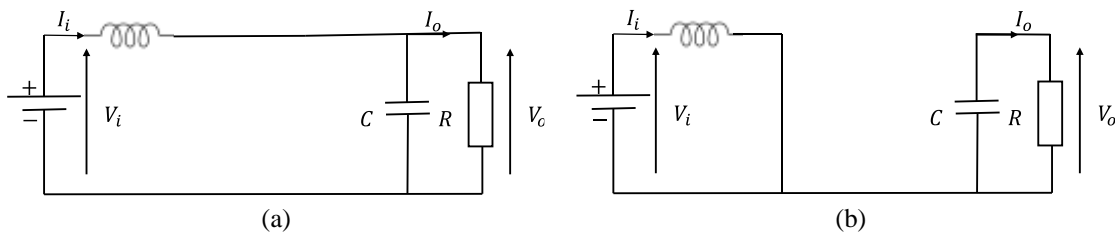

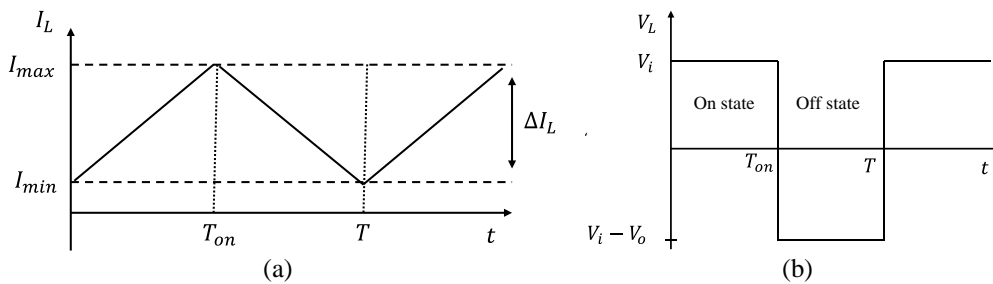Figure 5. Boost converter operating modes (a) ON mode and (b) OFF mode

Figure 6. Inductance behavior during switching (a) inductor voltage form and (b) inductance current form

− When switch Q is in the on state:

$$V_i = L\frac{di_L}{dt} \tag{6}$$

$$\Delta i_L{}^{(Ton)} = \frac{V_i}{L}\int_0^{Ton} dt = \frac{V_i}{L}T_{on} \tag{7}$$

− When switch Q in the off state:

$$V_I = L\frac{di_L}{dt} + V_O \tag{8}$$

$$\Delta i_L{}^{(T-Ton)} = \frac{1}{L}\int_{Ton}^T (V_i - V_O)dt = \frac{V_i - V_O}{L}(T - Ton) \tag{9}$$

Since switching is continuous according to the hypothesis, then the current flowing through the inductor when the switch is in the on state will start to flow away from the inductor in the off state. Since switching is continuous according to the hypothesis, then the current flowing through the inductor when the switch is in the on state will start to flow away from the inductor in the off state. Which mathematically expresses:

$$\Delta i^{(T_{on})} + \Delta i^{(T-T_{on})} = 0 \tag{10}$$

After a brief calculation, we find the expression that characterizes the operation of the boost converter according to the proposed hypothesis:

$$\frac{V_i}{V_o} = \frac{T}{T-T_{on}} = \frac{1}{1-D} \tag{11}$$

it is obvious then that the voltage output of this converter can only be greater than or equal to the input voltage. Boost converter parameters such as input and output inductance and capacitance can be calculated using the following relationships [25]:

$$L \geq \frac{V_i D}{f_s \Delta I_L} \tag{12}$$

$$C \geq \frac{V_o D}{f_s R \Delta V_o} \tag{13}$$

2.3. MPPT controllers modelling

The objective of MPPT control is to extract the maximum power from a PV system during changes in irradiance or connected load, i.e., to optimize the production of electrical energy. MPPT controllers differ in terms of complexity, speed and performance. In this section, we will study the basic concept of the controllers proposed for this work, P&O controller and FLC [10].

2.3.1. Perturb and observe concept

The basic concept of the P&O control for MPPT in PV systems is to perform a disturbance, that is, to apply small disturbances in the voltage or current output of the solar panel, and then observe how the disturbance affects the output power. Finally, adjust the voltage or current in the direction that resulted in an increase in power, aiming to reach the maximum power point [10], [11]. The Figure 7 shows the concept of the P&O algorithm based on $\frac{\Delta P}{\Delta V}$ slope calculation.
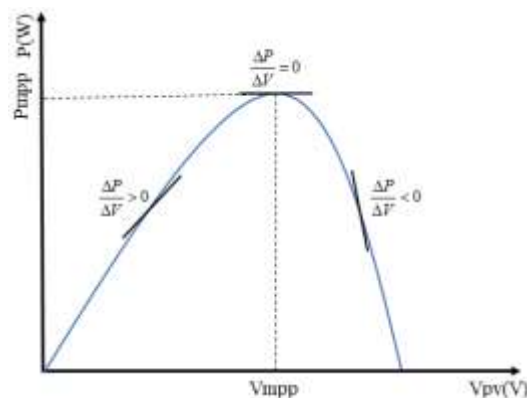

Figure 7. Solar panel PV characteristics [11]

After acquiring and measuring the solar system's voltage V_{pv} and current I_{pv}, the controller proceeds to the step of calculating the slope $\frac{dP}{dV}$. The sign of this slope allows the controller to determine the direction of the power evolution P_{pv}. Then, the controller moves to the conditional structure step, which enables it to

make decisions based on the slope's sign in each iteration. The flowchart in the Figure 8 illustrates the structure of our proposed P&O controller.
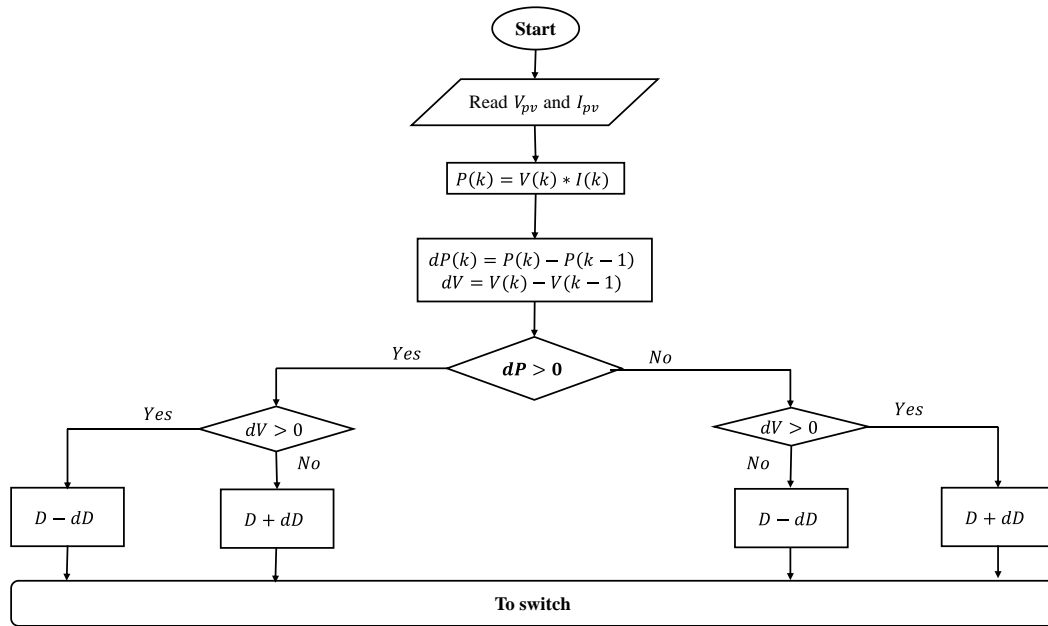

Figure 8. P&O controller flowchart [11]

2.3.2. Fuzzy logic controller concept

A FLC uses fuzzy logic, which allows data and conditions to be processed in a less rigid more intelligent way than conventional binary logic. Instead of simple "true" or "false", it uses fuzzy sets with degrees of membership. It is based on concepts such as fuzzy sets, membership functions, fuzzy rules, fuzzy inference, aggregation and defuzzification. This type of controller is used for decision-making in systems with vague, uncertain or qualitative data [9], [16], [27]. Our work is based on the general structure of a fuzzy controller illustrated in Figure 9.
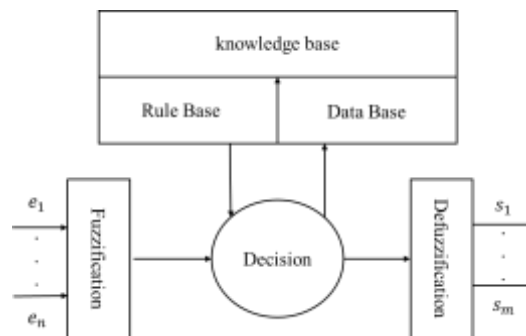

Figure 9. Structure of a fuzzy controller [9]

The structure of a typical fuzzy controller generally comprises the following components [27]:
− Fuzzy inputs: these are the system variables that the fuzzy controller takes into account when making decisions. In our application, the FL controller inputs are:

$$E(k) = \frac{P(k) - P(k-1)}{V(k) - V(k-1)} \tag{14}$$

$$CE(k) = E(k) - E(k) \tag{15}$$

- Fuzzification: the fuzzification process consists in converting the precise values of input variables according to (14) and (15) into fuzzy sets. This makes it possible to deal with the uncertainty and subjectivity associated with these values. Each input variable is associated with relevant fuzzy sets in the fuzzy database.
- Knowledge base: the knowledge base is a more general term that can include both the fuzzy database and the rule base. It is the body of information used by the fuzzy controller to make decisions.
- Data base: the fuzzy database contains the fuzzy sets that describe the different states or levels of the input variables. These fuzzy sets define linguistic terms such as "very hot", "medium", and "very low".
- Rule base: these are fuzzy rules describing the relationship between system inputs and outputs. These rules are usually expressed as "IF [condition] THEN [conclusion]".
- Rule aggregation: the degrees of truth of the various rules are combined to obtain a single value representing the global activation of the rules.
- Defuzzification: the defuzzification process converts the activated fuzzy sets of output variables into precise values. This gives a crisp response that the system can use to perform concrete actions.
- Decision: the final decision is based on the defuzzied value of the output variables. This is the concrete output that will be used to control the system.
- Fuzzy outputs: these are the variables that the fuzzy controller adjusts according to its decisions.

In our application, the fuzzy controller input variables are the voltage V_{pv} and the power P_{pv}, and the output is the duty cycle D. The processing procedure then follows the architecture described above, the Figure 10 illustrates the membership functions of the input and output variables of our proposed fuzzy controller. Figure 10(a) shows membership functions associated with input $E(k)$, Figure 10(b) shows membership functions associated with input $CE(k)$, and Figure 10(c) membership functions associated with input $D(k)$. The block containing the knowledge base and the decision in our fuzzy controller architecture is summarized in the Table 1.
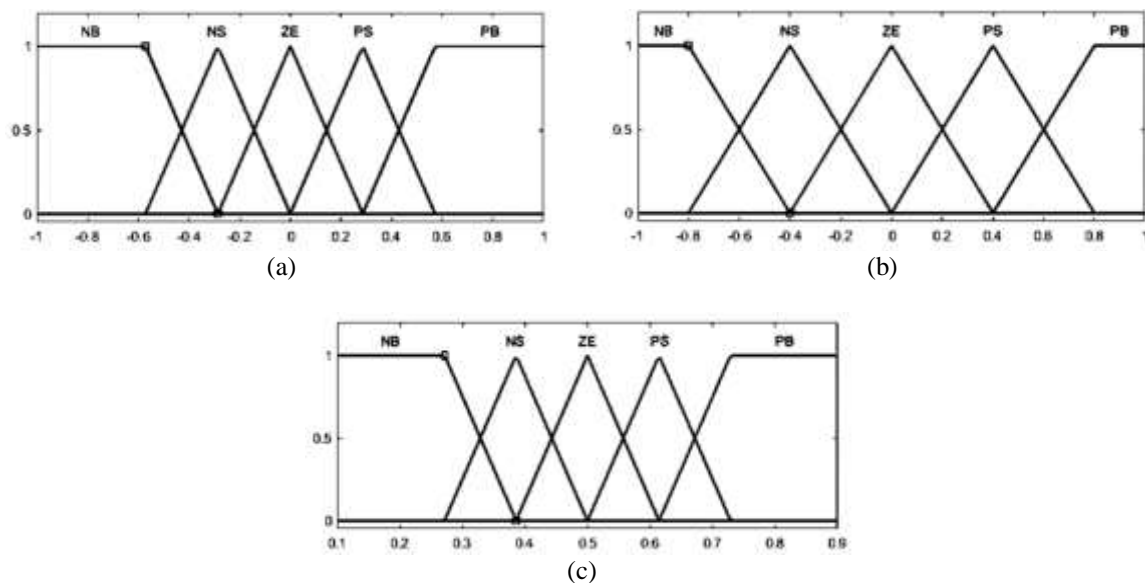

(a)   (b)

(c)

Figure 10. Fuzzy logic input/output membership function graphs; (a) error, (b) error variation, and (c) duty cycle [27]

Table 1. Table of inference rules [9], [16]

E	CE				
	Negative big (NB)	Negative small (NS)	Xero (ZE)	Positive small (PS)	Positive big (PB)
NB	ZE	ZE	NB	NB	NB
NS	ZE	ZE	NS	NS	NS
ZE	NS	ZE	ZE	ZE	PS
PS	PS	PS	PS	ZE	ZE
PB	PB	PB	PB	ZE	ZE

3. SPECIFICATIONS

In this work, we chose a 20-Watt solar panel to test the performance of our proposed controllers. The solar panel characteristics of this prototype are shown in Figure 1 and Table 2. The values of the parameters that the boost inverter must take are necessarily required by the solar panel, the connected load and the switching frequency imposed by the controller. Based on this reasoning.

Before moving on to simulation and implementation, we tested the operation of our converter according to the specifications imposed by the solar system under study. The Figure 11 illustrates the test by simulation and implementation of the boost converter with an input voltage of 15 volts and a duty cycle of 50%. Figure 11(a), is a boost converter simulation on MATLAB/Simulink under the given specifications on the Table 3, and Figure 11(b), is the realization of this converter. We have validated the operation of our converter in simulation and in realization according to the imposed specifications.

Table 2. Studied panel parameters

Parameter	Value	Unit
Open circuit voltage V_{oc}	28.8	Volt
Voltage at maximum power point V_{mpp}	18.7	Volt
Short circuit current I_{sc}	1.15	Ampere
Current at maximum power point I_{mpp}	1.07	Ampere
Maximum power P_{mpp}	20.0	Watt

Table 3. Boosting converter parameters examined

Parameter	Value	Unit
Swiching frequancy f_s	50	KH
Inductor L	2	mH
Output Capacitor C	400	uF
DC load R	100	Ohm
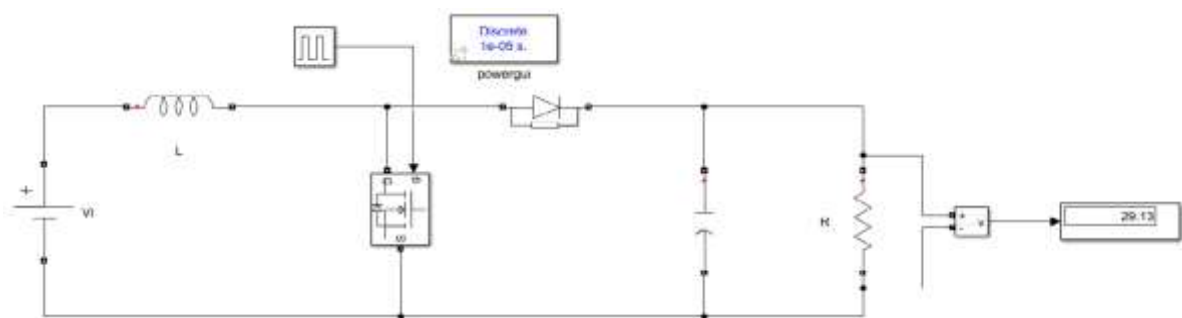
(a)
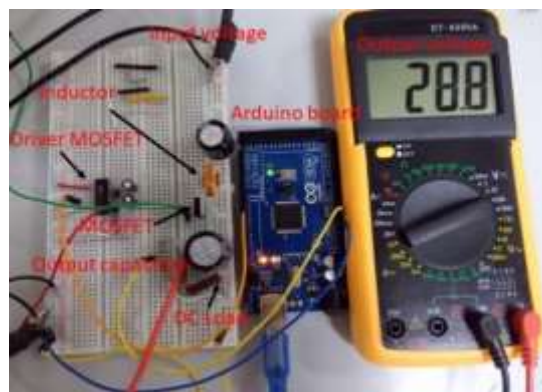
(b)

Figure 11. Simulation and boost converter testing (a) boost converter simulation and (b) boost converter realization

4. SIMULATION AND RESULTS

In this section, we aim to test the efficiency and preferences of our proposed controllers using the MATLAB/Simulink environment. We tested the system under different illumination conditions and connected loads neglecting the effect of temperature on the efficiency of the system studied, first taking two illumination values $I_{rr} = 1,000 \, w/m^2$ and $I_{rr} = 500 \, w/m^2$ with a load of $R = 100 \, \Omega$ Ohms, then we tested the load variation under maximum illumination ($I_{rr} = 1,000 \, w/m^2$), taking $R_1 = 200 \, \Omega$ and $R_2 = 100 \, \Omega$. This test was carried out for both controllers P&O and FLC in parallel. The Figure 12 shows the overall system simulation on MATLAB/Simulink containing the electrical and control parts as described above. The MATLAB/Simulink simulation of the FLC and P&O controllers for the MPPT are briefly shown in Figures 13 and 14.
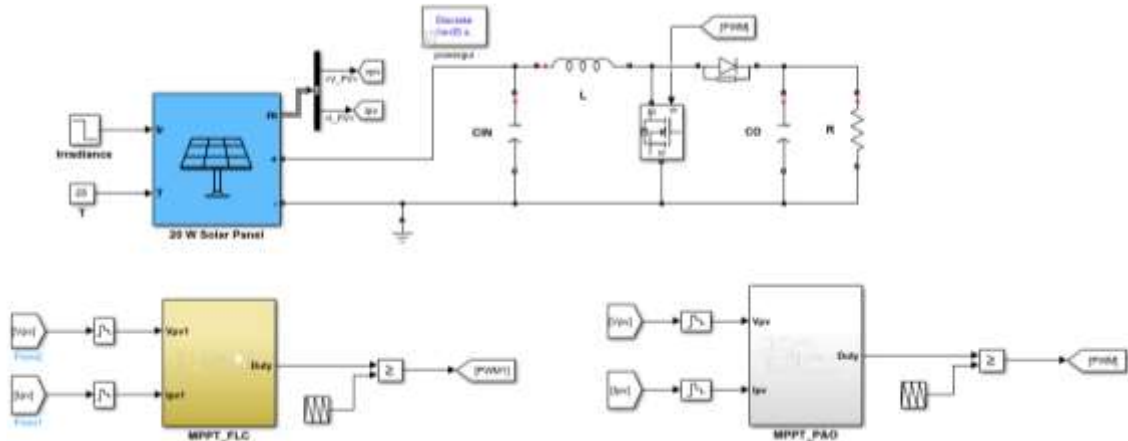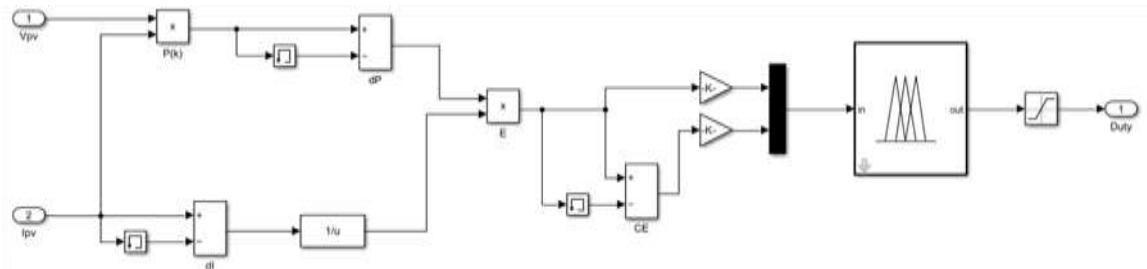

Figure 12. System simulation
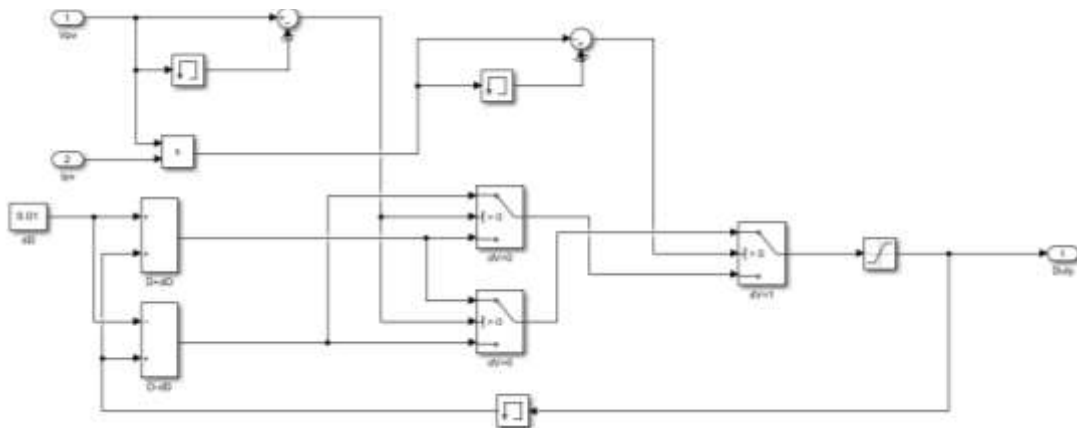

Figure 13. Fuzzy logic controller simulation

Figure 14. P&O controller simulation

4.1. Test by irradiation variation

Figure 15 shows the power shape of the power extracted from the photovoltaic system in the irradiance variation test, as Figure 15(a) illustrates the power shape produced P_pv by the system under FLC control, and Figure 15(b) represents the power produced by the system under P&O control. Figure 16 illustrates the voltage shape V_pv of this system in this test, as Figure 16(a) illustrates the voltage shape applied to the terminals of our system under FLC control, and Figure 16(b) illustrates the voltage shape applied to the terminals of our system under P&O control. In Figure 17, the current P_pv delivered by our system is illustrated in this test, as Figure 17(a) illustrates the current shape of our system under FLC control, and Figure 17(b) illustrates the current shape under P&O control. The system starts with an irradiance of 1,000 W/m², after a duration of 250 ms, the irradiance is changed to 500 W/m².
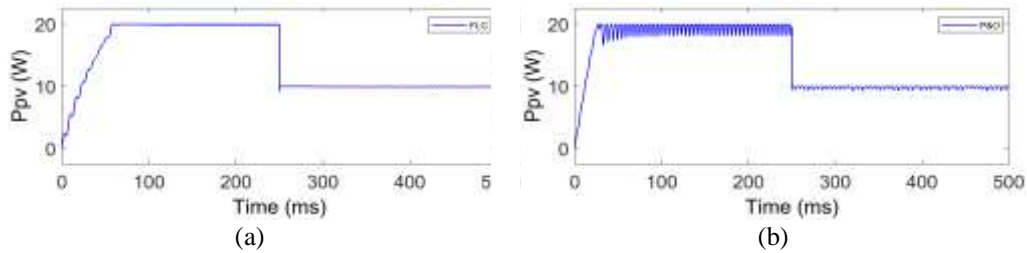

(a)   (b)

Figure 15. PV system power in irradiation variation (a) power for FLC and (b) power for P&O

(a)   (b)
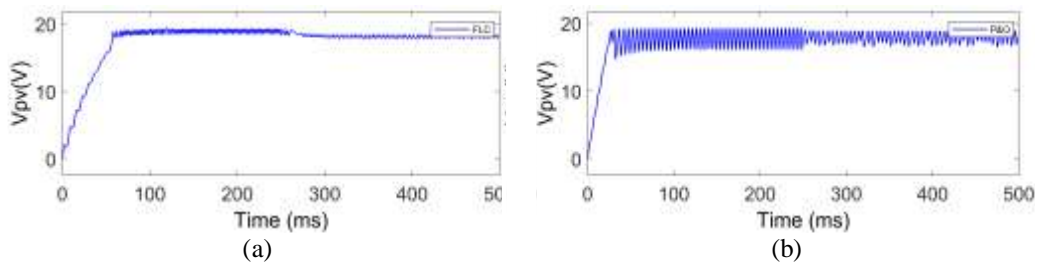
Figure 16. PV system voltage in irradiation variation (a) voltage for FLC and (b) voltage for P&O

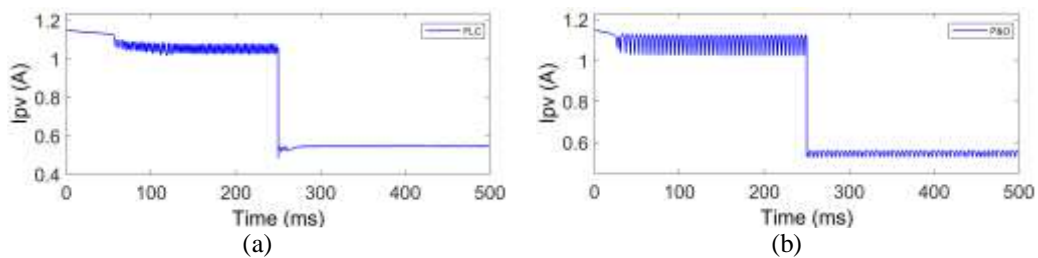(a)   (b)

Figure 17. PV system current in irradiation variation (a) current for FLC and (b) current for P&O

4.2. Test by load variation

Figure 18 shows the power shape of the power extracted from the photovoltaic system in the irradiance variation test, as Figure 18(a) illustrates the power shape produced P_{pv} by the system under FLC control, and Figure 18(b) represents the power produced by the system under P&O control. Figure 19 illustrates the voltage shape V_{pv} of this system in this test, as Figure 19(a) illustrates the voltage shape applied to the terminals of our system under FLC control, and Figure 19(b) illustrates the voltage shape applied to the terminals of our system under P&O control. In Figure 20, the current P_{pv} delivered by our system is illustrated in this test, as Figure 20(a) illustrates the current shape of our system under FLC control, and Figure 20(b) illustrates the current shape under P&O control. The system starts with a load of 200 Ohms, after 250 ms, the load is changed to 100 Ohms.
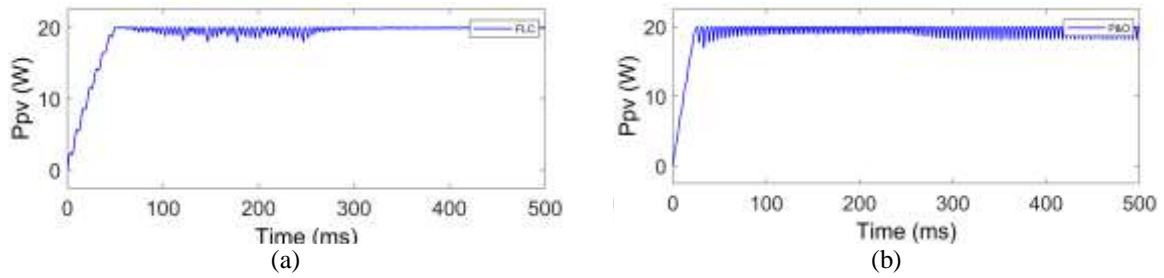
Figure 18. PV system power in load variation (a) power for FLC and (b) power for P&O
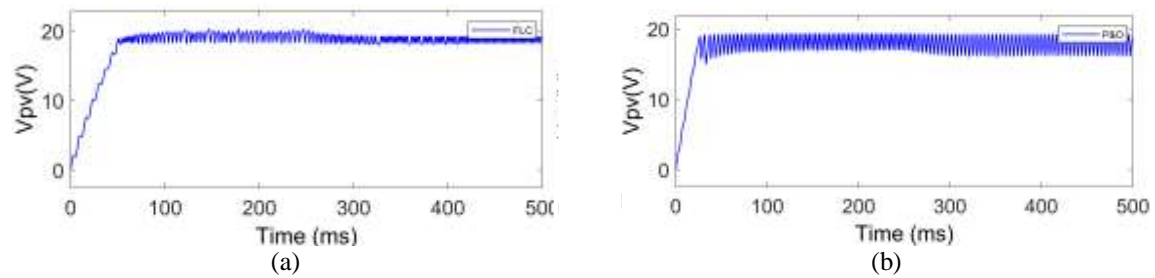

Figure 19. PV system voltage in load variation (a) voltage for FLC and (b) voltage for P&O
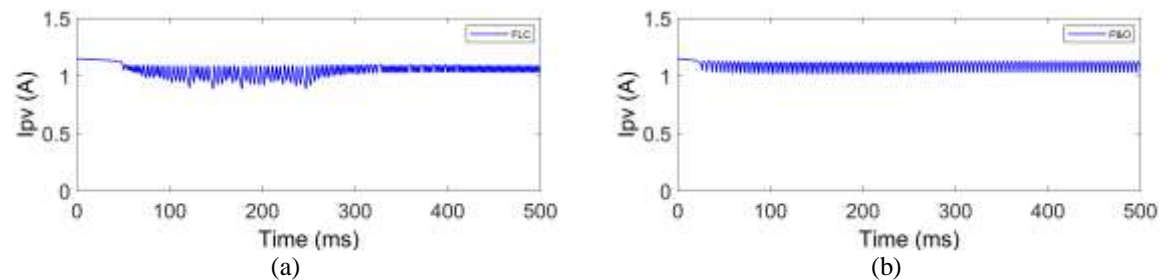

Figure 20. PV system current in load variation (a) current for FLC (b) current for P&O

5.   REALIZATION AND RESULTS

We carried out a test using the system studied, implementing in succession the two algorithms proposed in this study. The test was carried out in a real climate with maximum irradiation and an intermediate temperature close to 25 °C. In this test, temperature had no effect on system operation. The implementation was carried out using an Arduino Mega board and the Simulink support package for Arduino library, which is integrated into the MATLAB/Simulink environment. This option helped us to implement and monitor system behavior and power output in real time. Real-time acquisition of current Ipv and voltage Vpv is performed by a current sensor and a voltage sensor with good accuracy. During system operation, the power curve produced by the system was visualized in real time using the Arduino board interfacing option in the Simulink environment. The Figure 21 shows the experimental device of the system studied in the test moment. For the implementation of the MPPT controllers studied, we are keeping the same structures as we established in the simulation part, except that we're adding blocks that define the inputs for acquisition and the outputs for control connected to the Arduino board.

The Figure 22 shows the MPPT FL algorithm implemented on the Arduino board after input and output pins have been added. In the test moment, we recorded the evolution of power produced in real time by the system under the successive control of the two algorithms FLC and P&O. The Figure 23 illustrates our results obtained during this test, such that Figure 23(a) shows the power extracted using the P&O controller and Figure 23(b) shows the power extracted using the FLC controller.

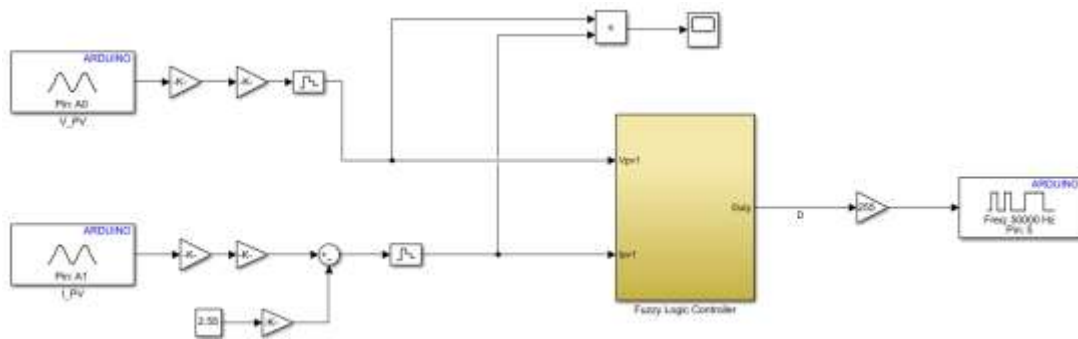Figure 21. Prototype of system studied under maximum illumination

Figure 22. Fuzzy logic-based MPPT control implemented on the Arduino Mega 2560 board

| (a) | (b) |
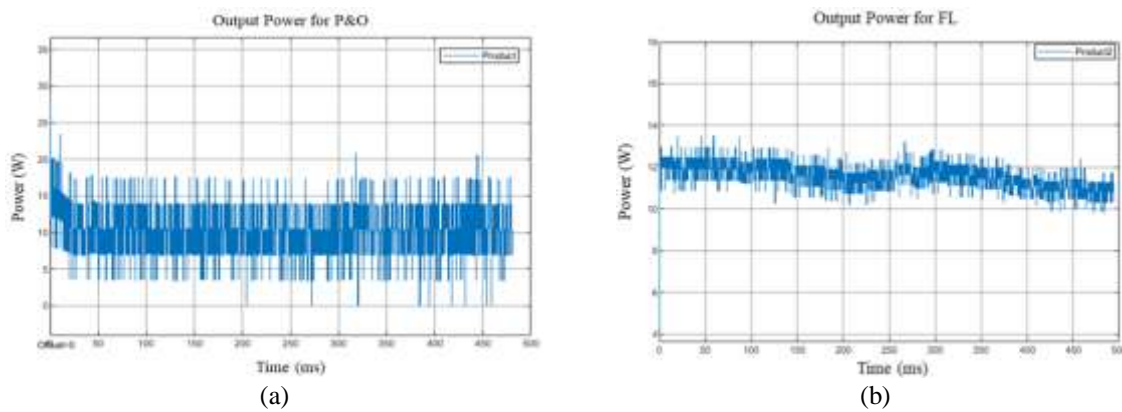
Figure 23. Practical implementation results at under maximum illumination (a) power with MPPT FL and (b) power with MPPT P&O

6. DISCUSSION

The results obtained from the simulation test show that there is a big difference between the two algorithms studied in terms of performance and power quality. The P&O algorithm has a generally admissible operation but performs less well because it represents oscillations author of optimal point, this oscillation responds to the operating state of the system, so it linked essentially to variations in irradiation and load, then the system under the control of P&O, can perform if the operating conditions are more limited which is undesirable realization under real conditions. Otherwise, the efficiency of the FLC algorithm is higher under both test conditions, whereas with the P&O algorithm, oscillation is much reduced and not influenced by changing irradiance and load, and the FLC controller is faster and more accurate and has a

wider control range than the P&O one. In the realization test, it is clear that the system performs better under FLC control than under P&O control (response time less than 0.1 s). Under the same operating conditions, it is clear that the FLC controller reduced oscillations better than the P&O controller. Therefore, it is clear that the FLC controller has improved system performance more than the P&O controller. By analogy with other work in this context, Azad et al. [13] tested the validity of the INC algorithm and found that it performs well under variable weather conditions, but is still slower (on the order of 0.2 second) and has more maximum point author oscillation than the FL algorithm. Hoang and Le [18] also found that the PSO algorithm performs well, but its convergence speed is relatively slow (on the order of 0.87 second). It is clear then that the FL algorithm we have studied and implemented for the power maximization of this installation is more optimal in terms of speed, performance, accuracy and reliability than the traditional P&O algorithm we have treated as a reference, and the INC and PSO algorithms for other works we have cited.

7. CONCLUSION

In summary, our research focused mainly on the study, simulation and practical implementation of a fuzzy logic and P&O based MPPT controller with the aim of optimizing the performance of power generation systems (solar panels). Through simulation testing, we found that the fuzzy logic-based controller performed better than the P&O algorithm under all operating conditions, including dynamic response, MPPT accuracy and overall energy efficiency. These results highlight the effectiveness and potential of the fuzzy logic approach for improving the performance of solar energy systems. Although the fuzzy logic-based MPPT controller has proved to be a promising technique, there is still room for improvement. One possible avenue is to investigate advanced fuzzy logic methods such as adaptive fuzzy logic, hybrid fuzzy logic with sliding mode or with neuron networks, or by implementing other more intelligent control techniques such as neural networks or genetic algorithms to improve MPPT tracking performance. However, it is important to note that practical implementation of the fuzzy logic-based MPPT controller on real solar systems would require additional cost-benefit analysis compared to other MPPT control techniques. Finally, future studies may be of interest, such as improving MPPT controllers by implementing adaptive, robust, intelligent and hybrid algorithms, as well as applying the fuzzy logic concept to other electrical systems such as wind turbines, and electrical vehicles.

REFERENCES

[1] D. Abbott, "Keeping the energy debate clean: how do we supply the world's energy needs?," *Proceedings of the IEEE*, vol. 98, no. 1, pp. 42–66, Jan. 2010, doi: 10.1109/JPROC.2009.2035162.
[2] Ü. Ağbulut and S. Sarıdemir, "A general view to converting fossil fuels to cleaner energy source by adding nanoparticles," *International Journal of Ambient Energy*, vol. 42, no. 13, pp. 1569–1574, Oct. 2021, doi: 10.1080/01430750.2018.1563822.
[3] F. A. Syam, M. I. A. El-Sebah, K. S. Sakkoury, and E. A. Sweelem, "Operation of biogas-solar-diesel hybrid renewable energy system with minimum reserved energy," *Indonesian Journal of Electrical Engineering and Computer Science*, vol. 28, no. 3, pp. 1203–1213, Dec. 2022, doi: 10.11591/ijeecs.v28.i3.pp1203-1213.
[4] Y. F. Makogon, "Natural gas hydrates-a promising source of energy," *Journal of Natural Gas Science and Engineering*, vol. 2, no. 1, pp. 49–59, Mar. 2010, doi: 10.1016/j.jngse.2009.12.004.
[5] H. Cheng and Y. Hu, "Municipal solid waste (MSW) as a renewable source of energy: current and future practices in China," *Bioresource Technology*, vol. 101, no. 11, pp. 3816–3824, Jun. 2010, doi: 10.1016/j.biortech.2010.01.040.
[6] R. Williams, "Becquerel photovoltaic effect in binary compounds," *The Journal of Chemical Physics*, vol. 32, no. 5, pp. 1505–1514, May 1960, doi: 10.1063/1.1730950.
[7] C. Leroy and P.-G. Rancoita, *Principles of radiation interaction in matter and detection*, 3rd edition. World Scientific, 2011.
[8] A. Chatterjee, A. Keyhani, and D. Kapoor, "Identification of photovoltaic source models," *IEEE Transactions on Energy Conversion*, vol. 26, no. 3, pp. 883–889, Sep. 2011, doi: 10.1109/TEC.2011.2159268.
[9] A. M. Noman, K. E. Addoweesh, and H. M. Mashaly, "A fuzzy logic control method for MPPT of PV systems," in *IECON 2012-38th Annual Conference on IEEE Industrial Electronics Society*, Oct. 2012, pp. 874–880, doi: 10.1109/IECON.2012.6389174.
[10] A. S. Ahmed, B. A. Abdullah, and W. G. A. Abdelaal, "MPPT algorithms: performance and evaluation," in *2016 11th International Conference on Computer Engineering and Systems (ICCES)*, Dec. 2016, pp. 461–467, doi: 10.1109/ICCES.2016.7822048.
[11] *M. L. Azad, P. K. Sadhu, and S. Das, "Comparative Study between PO and Incremental Conduction MPPT Techniques- A Review," Proceedings of International Conference on Intelligent Engineering and Management, ICIEM 2020, pp. 217–222, Jun. 2020, doi: 10.1109/ICIEM48762.2020.9160316.*
[12] H. M. A. Alhussain and N. Yasin, "Modeling and simulation of solar PV module for comparison of two MPPT algorithms (P&O and INC) in MATLAB/Simulink," *Indonesian Journal of Electrical Engineering and Computer Science (IJEECS)*, vol. 18, no. 2, pp. 666–677, May 2020, doi: 10.11591/ijeecs.v18.i2.pp666-677.
[13] M. L. Azad et al., "An efficient MPPT approach of PV systems: incremental conduction pathway," *Indonesian Journal of Electrical Engineering and Computer Science (IJEECS)*, vol. 15, no. 3, pp. 1189–1196, Sep. 2019, doi: 10.11591/ijeecs.v15.i3.pp1189-1196.
[14] E. Mamarelis, G. Petrone, and G. Spagnuolo, "Design of a sliding-mode-controlled SEPIC for PV MPPT applications," *IEEE Transactions on Industrial Electronics*, vol. 61, no. 7, pp. 3387–3398, Jul. 2014, doi: 10.1109/TIE.2013.2279361.
[15] E. Bianconi et al., "A fast current-based MPPT technique employing sliding mode control," *IEEE Transactions on Industrial Electronics*, vol. 60, no. 3, pp. 1168–1178, Mar. 2013, doi: 10.1109/TIE.2012.2190253.
[16] S. Yan, J. Yuan, and L. Xu, "Fuzzy logic control of MPPT for photovoltaic power system," in *2012 9th International Conference on Fuzzy Systems and Knowledge Discovery*, May 2012, pp. 448–451, doi: 10.1109/FSKD.2012.6234208.

[17] H. Renaudineau *et al.*, "A PSO-based global MPPT technique for distributed PV power generation," *IEEE Transactions on Industrial Electronics*, vol. 62, no. 2, pp. 1047–1058, Feb. 2015, doi: 10.1109/TIE.2014.2336600.

[18] T. T. Hoang and T. H. Le, "Application of mutant particle swarm optimization for MPPT in photovoltaic system," *Indonesian Journal of Electrical Engineering and Computer Science (IJEECS)*, vol. 19, no. 2, pp. 600–607, Aug. 2020, doi: 10.11591/ijeecs.v19.i2.pp600-607.

[19] Y. H. Liu, S. C. Huang, J. W. Huang, and W. C. Liang, "A particle swarm optimization-based maximum power point tracking algorithm for PV systems operating under partially shaded conditions," IEEE Transactions on Energy Conversion, vol. 27, no. 4, pp. 1027–1035, 2012, doi: 10.1109/TEC.2012.2219533.

[20] P. Q. Dzung, L. D. Khoa, H Lee, L. M. Phuong, and N. T. D. Vu, "The new MPPT algorithm using ANN-based PV," in *International Forum on Strategic Technology 2010*, Oct. 2010, pp. 402–407, doi: 10.1109/IFOST.2010.5668004.

[21] D. P. Mishra, R. Senapati, and S. R. Salkuti, "Comparison of DC-DC converters for solar power conversion system," *Indonesian Journal of Electrical Engineering and Computer Science (IJEECS)*, vol. 26, no. 2, pp. 648–655, May 2022, doi: 10.11591/ijeecs.v26.i2.pp648-655.

[22] K. K. Rout, D. P. Mishra, S. Mishra, S. Patra, and S. R. Salkuti, "Perturb and observe maximum power point tracking approach for microgrid linked photovoltaic system," *Indonesian Journal of Electrical Engineering and Computer Science (IJEECS)*, vol. 29, no. 2, pp. 635–643, Feb. 2023, doi: 10.11591/ijeecs.v29.i2.pp635-643.

[23] K. M. Bhargavi, N. S. Jayalakshmi, D. N. Gaonkar, A. Shrivastava, and V. K. Jadoun, "A comprehensive review on control techniques for power management of isolated DC microgrid system operation," IEEE Access, vol. 9, pp. 32196–32228, 2021, doi: 10.1109/ACCESS.2021.3060504.

[24] S. Öztürk, P. Poşpoş, V. Utalay, A. Koç, M. Ermiş, and I. Çadırcı, "Operating principles and practical design aspects of all SiC DC/AC/DC converter for MPPT in grid-connected PV supplies," *Solar Energy*, vol. 176, pp. 380–394, Dec. 2018, doi: 10.1016/j.solener.2018.10.049.

[25] R. W. Erickson and D. Maksimovic, *Fundamentals of power electronics*. Springer, 2003.

[26] M. Al-Greer, M. Armstrong, M. Ahmeid, and D. Giaouris, "Advances on system identification techniques for DC–DC switch mode power converter applications," *IEEE Transactions on Power Electronics*, vol. 34, no. 7, pp. 6973–6990, Jul. 2019, doi: 10.1109/TPEL.2018.2874997.

[27] J. Liu, *Intelligent control design and MATLAB simulation*. Singapore: Springer Singapore, 2018.

BIOGRAPHIES OF AUTHORS

Abdelaziz Youssfi ⓘ 🔗 SC C obtained his Master's degree in Renewable Energy Engineering and Energy Efficiency in 2021. Currently, he is preparing his thesis in Management, Optimization, and Control of electrical systems for renewable energies. He has worked as a part-time lecturer with 2 years of teaching experience. His research focuses on the modeling and control of power electronic converters, optimization of renewable energy conversion and injection systems, microgrids, smart grids, and improving energy quality. He is a member of the Engineering and Applied Physics research team. He can be contacted at email: abdelaziz.youssfi@usms.ma.

Abdelmounaim Alioui ⓘ 🔗 SC C has a Master's degree specializing in Energy and Environmental Engineering. He is passionate about renewable energy and the energy efficiency of buildings. He is currently preparing his thesis on energy efficiency and eco-friendly buildings based on carbon-free materials. His research focuses on experimental studies, optimization, and simulation of the thermal energy behavior of buildings. He can be contacted at email: abdelmounaim.aliouifpb@usms.ac.ma.

Ait El Kadi Youssef ⓘ 🔗 SC C obtained his Aggregation degree in Electrical Engineering and Power Electronics in 2000, followed by a postgraduate diploma in Energetics in 2004. He has completed a Ph.D. in Instrumentation, Measurements, Control, Characterization, and Modeling in 2016. He is now a teacher researcher at Sultan Moulay Slimane University He has worked as an Associate Professor with a making teaching experience of 26+ years. His research focuses on the modeling and control of electrical machines and power electronics converters, optimization of renewable energies conversion and injection systems, microgrids, smart grids and improvement of energy quality. He was a member of Microelectronics, Embedded Systems and Telecommunication research team. Currently, he is a member of Engineering and Applied Physics research team. He serves on the scientific committees of several international conferences and he has reviewed 90+ manuscripts since he is serving as an active reviewer for various indexed journals. He can be contacted at email: youssef.aitelkadi@usms.ma.